Journal of Hydroscience and Hydraulic Engineering
Vol. 22, No.2 November, 2004, 1-10

NUMERICAL SIMULATION OF BRAIDED STREAM FORMATION ON THE BASIS OF SLOPE-COLLAPSE MODEL

By

Masato Sekine

Professor, Department of Civil and Environmental Engineering, Waseda University, Tokyo, Japan

SYNOPSIS

The formation process of braided streams is examined in this paper. A numerical simulation model including a "slope-collapse model" was newly developed here. The "slope collapse model" is applied to treat special cases where the angle of local slope grows steeper than the angle of repose temporally in computation. In such cases, the slope has to be collapsed to maintain the angle to be equal to the angle of repose. Bank erosion and the front migration of alternate bars are the typical examples to which the model can be applied effectively. The main findings of this study are summarized as follows: (a) the multiple-row bars form in the initial stage of this process, (b) as the time goes on, such bars combine to each other, and a typical braided stream with emerged bars forms and it migrates downstream. The interaction between bed deformation and bank erosion is an important phenomenon to be investigated in this process.

INTRODUCTION

The reclamation and maintenance work of river space have been carried out in order to provide more space for a natural environment. When we accomplish these purposes, a thorough understanding of the self-forming mechanism of natural rivers and the establishment of the prediction technique of channel evolution process are indispensable. As is well known, river channels can be classified into the following three categories: a straight channel, a meandering channel and a braided channel. The number of studies has been still limited on the formation of braided channel in comparison with the studies of a straight channel or a meandering channel. The reason is probably that the formation mechanism of a braided stream is more complicated and has the chaotic feature. The channel migration, which is caused by a bank erosion, the confluence of each streams and the appearance of emerged bars are the important sub-process to be investigated here.

Some important studies have been done on this formation mechanism by several researchers, for example, Fujita, Akamatsu & Muramoto (1), Ashida, Egashira, Satofuka & Gotoh (2), and recently by Takebayashi, Egashira & Okabe (3), (4) and Kurabayashi & Shimizu (5). Fujita, Akamatsu & Muramoto (1) made the most practical contribution experimentally to the later research, and useful information was reported as experimental

data with some discussion of them.

Based on these studies, a numerical simulation model of this channel evolution has been recently developed. The model is constituted by several sub-models to evaluate (a) a flow velocity field, (b) a sediment transport rate and (c) the deformation of channel elevation. The "slope collapse model" was newly invented to treat the special case that the angle of local slope grows steeper than the angle of repose temporally in computation. This model is an extended version of the bank erosion model by Sekine (6) which is similar to the ones by Hasegawa (7), Nagata, Hosoda & Muramoto (8). In such a case, the slope is expected to collapse so as to maintain the local angle to be equal to or less than the angle of repose because such a slope is unrealistic and unstable. The migration of an alternate bar and the channel migration of braided stream caused by a bank erosion are the typical examples to which the model can be applied effectively. If such a collapse occurs in this numerical computation, the additional sediment transport rate is taken into account by using this model and then the bed deformation is evaluated. The formation process of braided streams is investigated in this study by means of numerical experiments under the condition of a multiple-row bar formation.

NUMERICAL SIMULATION MODEL

FLOW VELOCITY FIELD

Flow depth in a braided stream is expected to be so small in comparison with the channel width that the so-called "shallow water assumption" can be effective. Therefore, the set of shallow water equations are the governing equations to be solved numerically. The following individual solution techniques were adopted: (a) the Staggered grid system was applied, (b) the Adams-Bashforth Scheme for non-convective terms and the CIP Scheme for convective terms were adopted, (c) the cyclic boundary condition at both upstream and downstream ends, and the non-slip boundary condition at both side boundary were used.

SEDIMENT TRANSPORT RATE

In the present analysis, bedload was only taken into account as the type of sediment transport, and suspended load was neglected because of the range of tractive force. The bedload function which enables us to predict a sediment transport rate more accurately even on the steep slope whose local angle is close to the angle of repose in arbitrarily direction is needed in this computaion. Kovacs & Parker (9) developed the generalized vectorial bedload function as the extension of Bagnold's hypothesis. A similar function was developed approximately without depending upon such hypothesis, and is used in this study. The system of bedload functions is explained briefly here . The magnitude of the bedload vector can be evaluated by Meyer-Peter and Muller's equation:

$$| \vec{q}_B | = 8 \times \sqrt{RgD^3}\ (\tau^* - \tau_c^*)^{3/2} \tag{1}$$

where τ^* = magnitude of the dimensionless vector of tractive force. Moreover, each components of bedload transport rate in longitudinal and transverse direction is decomposed into on the basis of the equation of sliding motion:

$$\frac{1}{2}\rho C_D \frac{\pi D^2}{4} | \vec{u}_b - \vec{u}_p | (\vec{u}_b - \vec{u}_p) + \rho R g \frac{\pi D^3}{6} \vec{n}_{gt} - \mu \rho R g \frac{\pi D^3}{6} n_{g3} \vec{n}_p = 0 \tag{2}$$

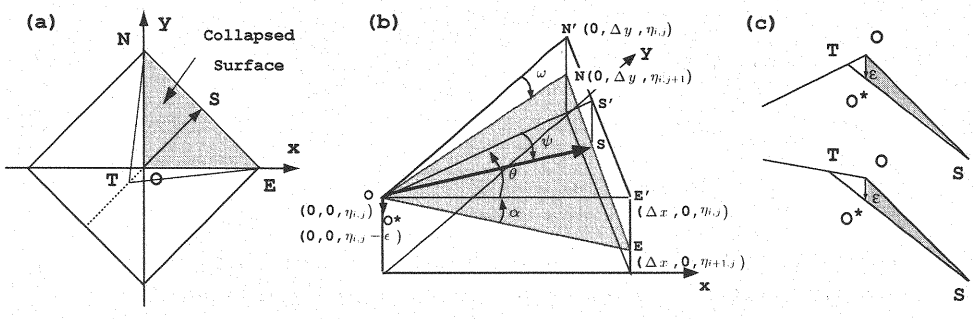

Fig. 1 Schematic explanation of the slope-collapse model:
(a) plane view, (b) a bird's-eye view of the steepest plane, (c) vertical view

where D = sediment diameter, R = submerged specific gravity of sediment, μ = static friction coefficient ($=\tan\phi$), ϕ = angle of repose, C_D= drag coefficient, and $\vec{u_b}$ or $\vec{u_p}$ = velocity vector of water or sediment, respectively. The vector $\vec{n}_p$ and $\vec{n}_g$ are the unit vectors in the directions of sediment transport and gravity on the bed surface respectively.

SLOPE-COLLAPSE MODEL

A summary of the "slope-collapse model" is described here. Fig. 1 illustrates the idea of this model. Now let us concentrate on the four planes around point O in the respective quadrants, and discuss the case where the steepest slope is assumed to be in the first quadrant of Fig. 1 (a) and (b). If the direction of steepest slope is from point O to point S, then the vector $\vec{OS}$ is expressed by

$$\vec{OS} = (s^*\Delta x,\ (1-s^*)\Delta y,\ s^* z_e + (1-s^*)z_n)\ ; \qquad s^* = \frac{(\Delta y)^2\, z_e}{(\Delta x)^2\, z_n + (\Delta y)^2\, z_e} \tag{3}$$

where $z_e = \eta_{i+1,j} - \eta_{i,j} < 0$, $z_n = \eta_{i,j+1} - \eta_{i,j} < 0$, and $\eta_{i,j}$, $\eta_{i+1,j}$, $\eta_{i,j+1}$ are the vertical coordinates of the Points O, N and E in Fig. 1 (a), (b) respectively. Points N' and E' are the projected points on the hirizontal plane on which Point O exists. The maximum value of downward gradient $\tan\psi$ can be expressed by

$$\tan\psi = \sqrt{\tan^2\alpha + \tan^2\omega} \tag{4}$$

where $\tan\alpha$ and $\tan\omega$ are the local gradient of slope in x and y direction in Fig. 1, respectively. If $\tan\psi$ is greater than $\tan\phi$, the collapse occurs to maintain the maximum local angle ψ to be equal to or less than the angle of repose ϕ in water. In this case, the author predicted that erosion will occur and the bed elevation at this point O changes vertically by the amount of ϵ ;

$$\epsilon = \sqrt{(s^*\Delta x)^2 + (1-s^*)^2\,(\Delta y)^2} \times (\tan\psi - \tan\phi) \tag{5}$$

Due to this collapse, the block of sediment moves in a downward direction of the slope within the period of each time step in computation. In the present model, such sediment supply is thought to be treated as the additional sediment transport. The vector of this additional sediment transport is assumed to be parallel to the vector $\vec{OS}$. Thus, the components of this transport vector per unit width $\vec{q}_{Collapse}$ in x and y direction are expressed by

$$\vec{q}_{Collapse} = Q_{Collapse} \times \left(\frac{\cos\theta}{\Delta y}, \frac{\sin\theta}{\Delta x} \right) \tag{6}$$

$$Q_{Collapse} = \beta \times \frac{(1-\lambda)\,(\epsilon\,\Delta x\,\Delta y)}{6\,\Delta t} \tag{7}$$

$$\theta = \arctan\left(\frac{(1-s^*)\Delta y}{s^*\Delta x} \right) = \arctan\left(\frac{\tan\omega}{\tan\alpha} \right) \tag{8}$$

where λ = porosity, and β = the correction coefficient that means the ratio of the projected area of $\triangle$ *TEN* on the horizontal plane to that of $\triangle$ *OEN* in Fig. 1(a). This additional sediment transport vector is taken into account quantitatively in the prediction of channel deformation as follows: The bed elevation at each grid point is calculated by solving the so-called "Exner's equation, and then the sum of this additional sediment transport rate, if necessary, and the value evaluated by the bedload functions is introduced into this equation. The bank erosion, which corresponds to the case illustrated simply in the lower part of Fig.1 (c), can be also considered in this numerical computation.

FORMATION PROCESS OF BRAIDED STREAM

SUMMARY OF THE CONDITION

A numerical simulation of the braided stream formation was conducted as the application of the model explained in the previous section. The computational condition was set by referring to the experiment by Fujita, Akamatsu & Muramoto (1), and is summarized as follows: the length of experimental flume is 15 m, the initial channel slope is 1/50, the water discharge is 4.0 x 10^{-3} m^3/sec, and the uniform-sized sediment whose mean size is 1.05 mm was used as the bed material. The original experiment by Fujita was conducted in a flume with fixed vertical side walls. In this numerical experiment, on the other hand, a computation for the channel with erodable inclined side walls as well as one with vertical unerodible side walls were conducted under the same conditions except for this side wall condition. In the case where erodable side walls, the bank erosion is expected to occur, and the interaction between the bed deformation and the bank erosion has to be examined. In the present paper, the results obtained for the case with erodable side walls is discussed because the results under the same condition of fixed side wall as Fujita's experiment has been already shown in a previous paper (10).

The initial condition for bed elevation is as follows: the bed surface was set to be the uniformly inclined flat plane in a downstream direction, but the perturbation in the scale of a sediment diameter was superimposed on the surface. Therefore, the bed is "random bed". The generator of uniform random number was used in the numerical model to evaluate such perturbation. The initial channel geometry is trapezoidal whose water surface has a width of 1.81 m.

FORMATION PROCESS OF BRAIDED STREAMS WITH BANK EROSION

The formation process of braided streams with erodable inclined side walls is discussed in this section. The results of the numerical computation are shown in Figs. 2 - 8.

Figure 2 shows the evolutional pattern of bed deformation, and is the contour map of bed elevation at the time writen there. In this figure, the difference between a local bed elevation at each time and that of initial flat bed without perturbation is shown. Active erosion occurs in the black portion in this figure. The following

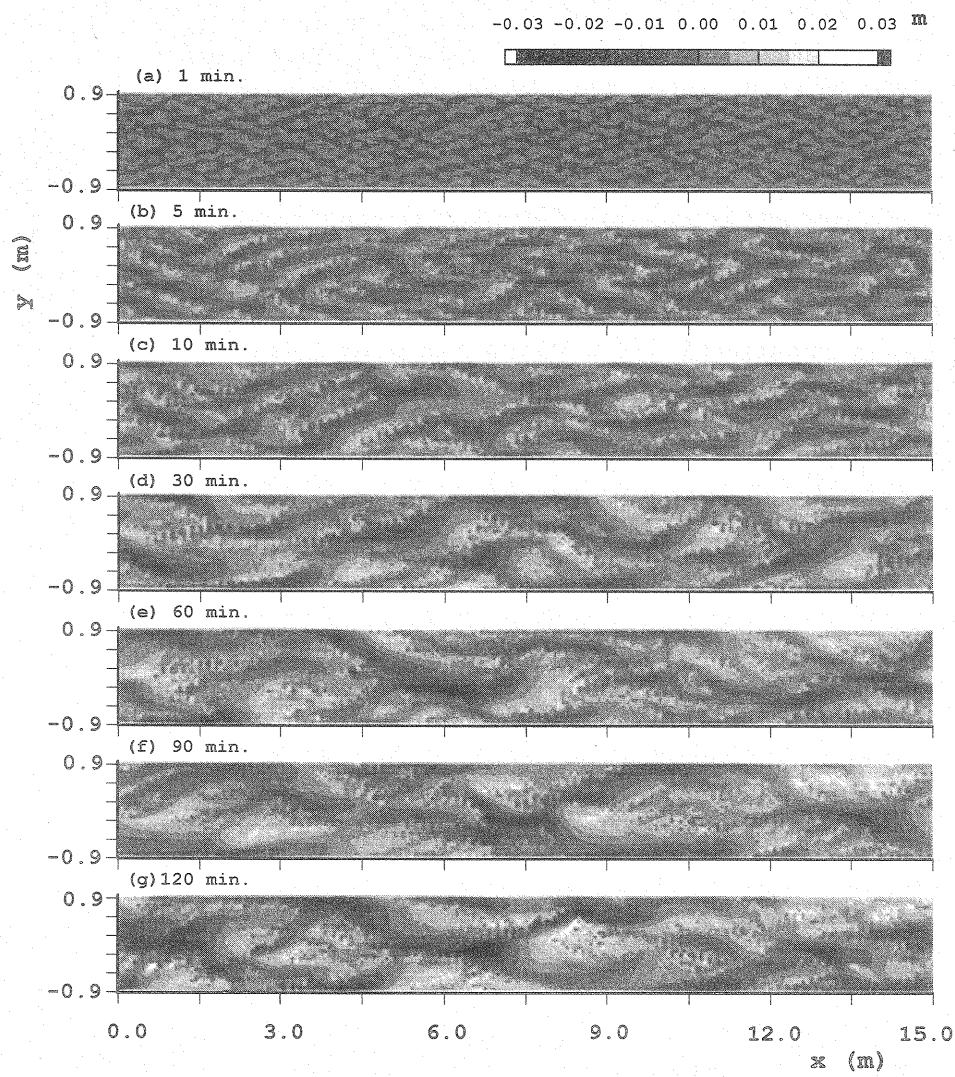

Fig. 2 Temporal variation of bed elevation

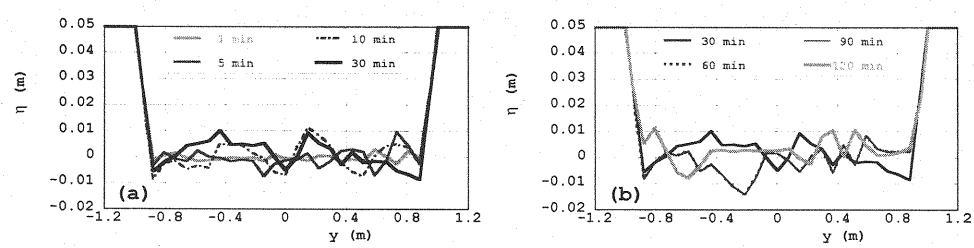

Fig. 3 Temporal variation of bed elevation in cross section at x = 7.5 (m) : (a) 1 - 30 min, (b) 30 - 120 min.

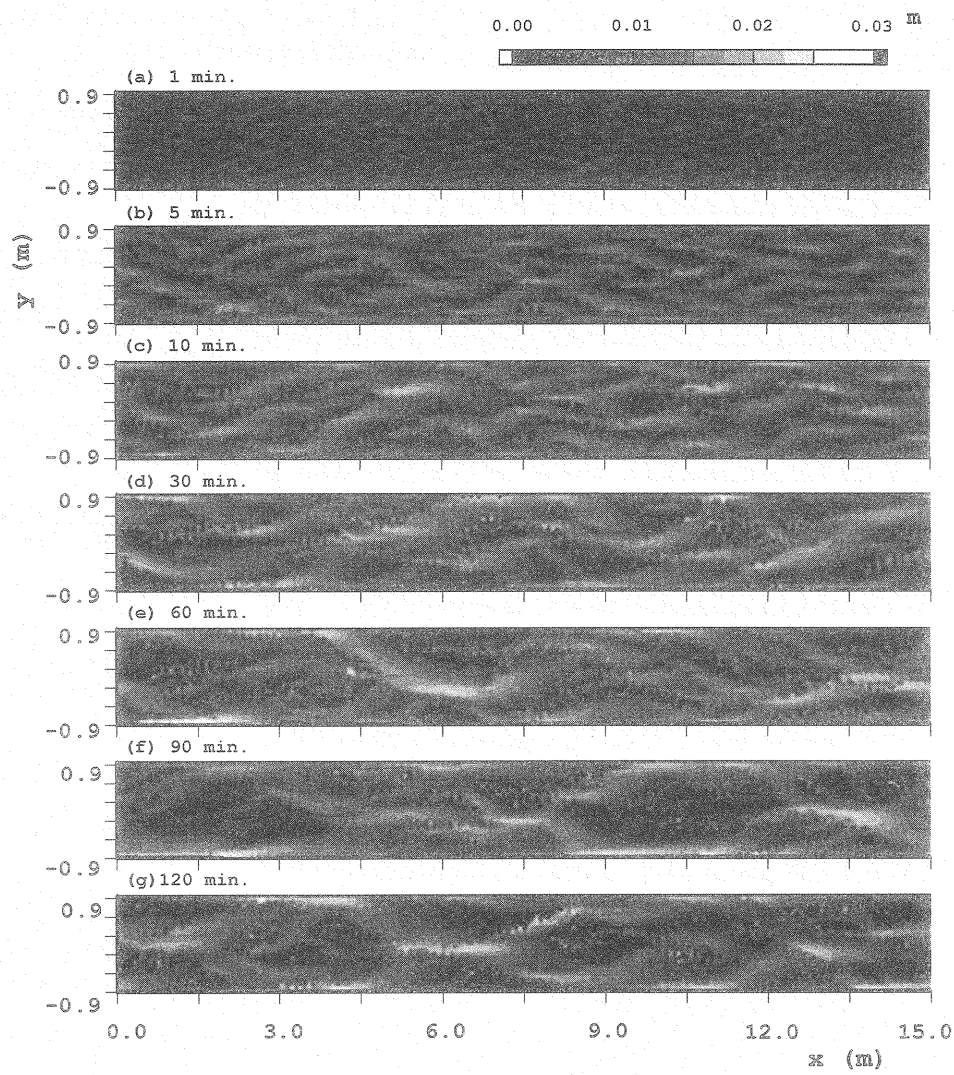

Fig. 4 Temporal variation of flow depth

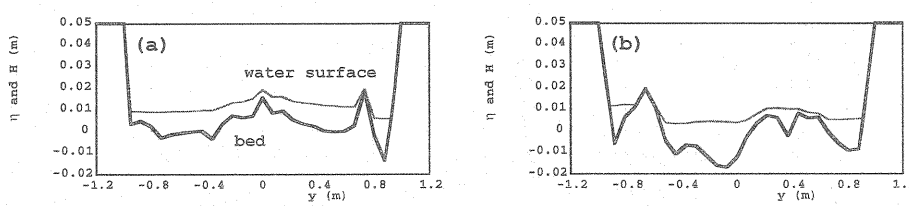

Fig. 5 Channel cross section at 120 min. : (a) x = 2.25 (m), (b) x = 6.0 (m)

findings were found: (i) the typical multiple-row bars form in the initial stage of this process (see Fig.2 (a)); (ii) as time passes, such bars disappear gradually, and then the larger-scale streams in both depth and width start forming which are caused by the merging of some smaller-scale streams (see Fig.2 (b)-(d)); and therefore the pattern of channel network becomes simpler than the initial one; (iii) some major streams survive, and the pattern of channels seem to migrate downstream with some deformation (see in Fig.2 (e)-(g)). It was observed that the "slope-collapse" occurs intermittently in the region far from the side bank as well as along the side bank, and the pattern of channels reach an almost complete equilibrium state in about 60 minutes, and then typical braided streams formed. Another aspect of bed deformation is shown in Fig. 3, which shows the temporal variation of channel cross section at x=7.5 (m). The vertical fluctuation of bed elevation was found to be about 0.01 m around the initial bed elevation during the period of this numerical experiment. It should be noted from Figs. 2 and 3 that the primary larger-scale channels tend to be located along the side wall, and the geometry of channel pattern shows just like a character "8" in downstream direction which is caused by the channel shift from one side to the other.

Figure 4 shows the temporal variation of contour map of flow depth. The white portion corresponds to the stream while black portion, in which the depth is 0 cm, to the emerged bar, the pattern of which is consistent with the result seen in Fig. 2. Two cross sections at x = 2.25 and 6.0 (m) are also shown in Fig. 5. In this figure, a water surface as well as the bed surface was drawn. It is also seen in this Fig. 5 that the emerged bars form in both cross sections.

Figure 6 shows the temporal variation of flow velocity vector. When focusing on the phenomenon 60 minutes after the beginning, for example, it was revealed that the braided stream crossed from one side to the other and hit the side wall, and then kept the location along the wall. Also, the velocity in the larger-scale stream is relatively higher. Therefore, the bank erosion arises around the point where the larger-scale stream hits the side wall.

In Fig. 7, the temporal variation of the lines of water margin on both side walls are shown. The contour maps in Figs. 2 and 4 or the velocity vector in Fig. 6 show the results only in the range bordered by the lines of initial water margin on side walls, that is , $-0.905 \leq y \leq 0.905$ (m). It can be seen from Fig.7 that the bank erosion, or the migration of water margin, occurs by the amount less than 10 cm. Furthermore, when comparing the lines in Fig. 7 with the contour maps of both bed elevation in Fig. 2 and water depth in Fig. 4, it can be concluded that the location where the bank erosion occurs is consistent with the location that the local scour has taken place. Moreover, due to the migration of emerged bars along the water margin, the location of the margin can sometimes shift toward the centerline of the channel.

Temporal variation of sediment transport rate was also analyzed, and the result is shown in Fig. 8. The vertical axis means the total bedload transport rate across the section of x = 15.0 (m). The fluctuation of sediment transport rate expresses the complexity of braided streams. Such fluctuation is correlates closely with the channel migration or disappearance.

CONCLUSION

The formation process of braided streams was investigated numerically in the present study. A "slope-collapse model" was developed for the first time so as to handle the unrealistically steep slope whose angle is greater than the angle of repose. In the case where such a steep slope occurs temporally in computation, the slope has to be collapsed to keep the angle be equal to the angle of repose. Therefore, this model was applied to the analysis of channel evolution process of braided streams in which the slope-collapsion of local bed and the bank erosion were observed numerically. A numerical simulation

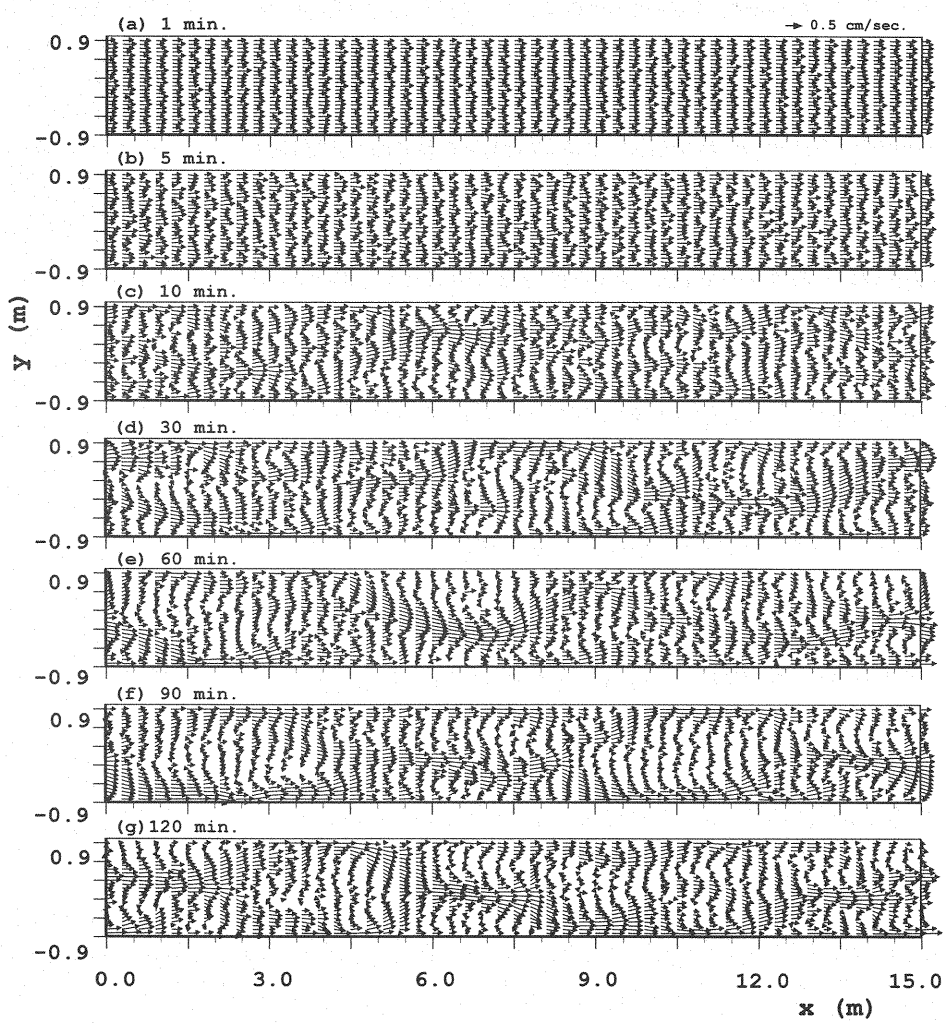

Fig. 6 Temporal variation of flow velocity vector

was conducted under the condition of a multiple-row bar formation. The main findings are summarized as follows: (a) multiple-row bars form in the initial stage, but are eroded and disappear gradually as time passes, (b) some major streams selectively survived, and the pattern of streams seems to become simpler, and they migrate downstream with some deformation, (c) the braided stream with relatively high velocity crosses from one side to the other and hits the side bank, and then the bank erosion occurs, (d) the pattern of bank erosion correlates closely with that of the local scour, (e) the major streams tend to be located along the side bank, and the geometry of channel network pattern is similar to the character "8" in downstream direction, (f) sediment transport rate has the tendency of fluctuating temporally under the effct of the channel evolution.

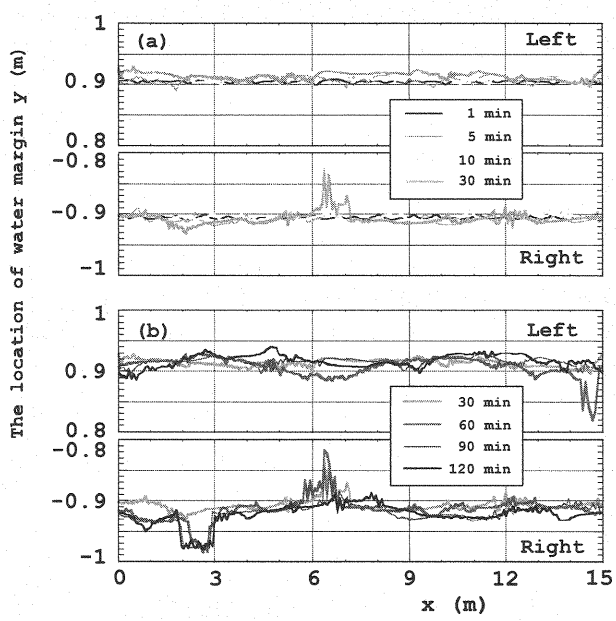

Fig. 7 Temporal variation of the line of water margin: (a) 1 - 30 min, (b) 30 - 120 min the upper half figure shows the left side margin, the lower shows the right side margin.

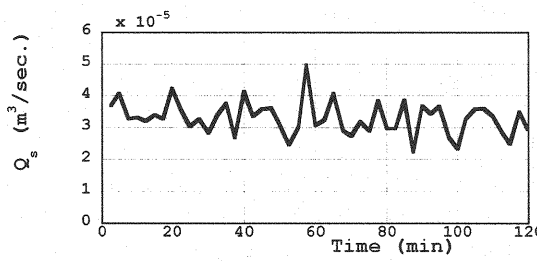

Fig. 8 Temporal variation of sediment transport rate

REFERENCES

1. Y. Fujita, H. Akamatsu and Y. Muramoto: Experiments on formative process of double row bars and braided streams, Annual Report of Disaster Prevention Research Institute, Kyoto University, No. 29 B-2, pp.451-472, 1986 (in Japanese).
2. K. Ashida, S. Egashira, Y. Satofuka and T. Gotoh: Variation of braided streams and sediment discharge, Annual Report of Disaster Prevention Research Institute, Kyoto University, No. 33 B-2, pp.241-260, 1990 (in Japanese).
3. H. Takebayashi, S. Egashira and T. Okabe: Stream formation process between confining banks of straight wide channels, 2nd IAHR Symposium on River, Coastal and Estuarine Morphodynamics, pp.575-584, 2001.

4. H. Takebayashi, S. Egashira and T. Okabe: Temporal and spatial variation characteristics of braided streams, Annual Journal of Hydraulic Engineering, JSCE, No. 46, pp.737-742, 2002 (in Japanese).
5. H. Kurabayashi and Y. Shimizu: Numerical calculations of bed deformation in braided stream with emerged mid-channel bars, Annual Journal of Hydraulic Engineering, JSCE, No. 46, pp.743-748, 2002 (in Japanese).
6. M. Sekine: Study on the channel migration due to a bank erosion, Journal of Hydraulic, Coastal and Environmental Engineering, JSCE, No.533 / II-34, pp.51-59, 1996 (in Japanese).
7. K. Hasegawa: Bank-erosion discharge based on a non-equilibrium theory, Proceedings of JSCE, No.316, pp.37-50, 1981 (in Japanese).
8. N. Nagata, T. Hosoda and Y. Muramoto: Characteristics of river channel processes with bank erosion and development of their numerical models, Journal of Hydraulic, Coastal and Environmental Engineering, JSCE, No.621 / II-47, pp.23-39, 1999 (in Japanese).
9. A. Kovacs and G. Parker: A new vectorial bedload formulation and its application to the time evolution of straight river channels, Journal of Fluid Mechanics, 267, pp.153-183, 1994.
10. M. Sekine: Numerical simulation of braided stream formation, Annual Journal of Hydraulic Engineering, JSCE, No. 47, pp.637-642, 2003 (in Japanese).

APPENDIX - NOTATION

The following symbols are used in this paper;

C_D = drag coefficient in Eq. 2;
D = sediment diameter;
$\vec{q}_{Collapse}$ = additional sediment transport vector;
$\vec{q}_B$ = bedload transport vector;
R = submerged specific gravity of sediment;
s^* = parameter in Eqs. 3, 5 and 8;
$\tan\alpha$ = local gradient of slope in streamwaise direction;
$\tan\omega$ = local gradient of slope in transverse direction;
$\tan\psi$ = maxmum gradient of slope;
$\vec{u_b}$ = velocity vector of water exerted on the sediment;
$\vec{u_p}$ = velocity vector of sediment;
β = the correction coefficient in Eq.7;
ϵ = virtual displacement by erosion at point O;
ϕ = angle of repose;
$\eta_{i,j}$ = bed elevation at node (i, j);
λ = porosity;
μ = static friction coefficient in Eq. 2;
θ = angle of additional sediment transport vector;
ρ = density of water;
τ^* = dimensionless tractive force; and
τ_c^* = dimensionless critical tractive force.

(Received June 30, 2003 ; revised March 30, 2004)